



## An Optimal Coordinated Method for EVs Participating in Frequency Regulation under Different Power System Operation States

Li, Canbing; Zeng, Long; Zhou, Bin; Liu, Xubin; Wu, Qiuwei; Zhang, Di; Huang, Sheng

*Published in:*  
IEEE Access

*Link to article, DOI:*  
[10.1109/ACCESS.2018.2875929](https://doi.org/10.1109/ACCESS.2018.2875929)

*Publication date:*  
2018

*Document Version*  
Peer reviewed version

[Link back to DTU Orbit](#)

*Citation (APA):*

Li, C., Zeng, L., Zhou, B., Liu, X., Wu, Q., Zhang, D., & Huang, S. (2018). An Optimal Coordinated Method for EVs Participating in Frequency Regulation under Different Power System Operation States. *IEEE Access*, 6, 62756-62765. DOI: 10.1109/ACCESS.2018.2875929

---

### General rights

Copyright and moral rights for the publications made accessible in the public portal are retained by the authors and/or other copyright owners and it is a condition of accessing publications that users recognise and abide by the legal requirements associated with these rights.

- Users may download and print one copy of any publication from the public portal for the purpose of private study or research.
- You may not further distribute the material or use it for any profit-making activity or commercial gain
- You may freely distribute the URL identifying the publication in the public portal

If you believe that this document breaches copyright please contact us providing details, and we will remove access to the work immediately and investigate your claim.

Date of publication xxxx 00, 0000, date of current version xxxx 00, 0000.

Digital Object Identifier 10.1109/ACCESS.2017.Doi Number

# An Optimal Coordinated Method for EVs Participating in Frequency Regulation under Different Power System Operation States

Canbing Li<sup>1,2</sup>, Senior Member, IEEE, Long Zeng<sup>1,2</sup>, Bin Zhou<sup>1,2</sup>, Senior Member, IEEE, Xubin Liu<sup>1,2</sup>, Qiuwei Wu<sup>3</sup>, Senior Member, IEEE, Di Zhang<sup>1,2</sup>, Student Member, IEEE, Sheng Huang<sup>3</sup>

<sup>1</sup>Hunan Key Laboratory of Intelligent Information Analysis and Integrated Optimization for Energy Internet, Hunan University, Changsha 410082.

<sup>2</sup>College of Electrical and Information Engineering, Hunan University, Changsha 410082.

<sup>3</sup>Center for Electric Power and Energy, Department of Electrical Engineering, Technical University of Denmark, Kgs. Lyngby, DK 2800.

Corresponding author: Bin Zhou (e-mail: binzhou@hnu.edu.cn).

This work is supported by Sino-US International Science and Technology Cooperation Project under Grant. (2016YFE0105300).

**ABSTRACT** This paper proposes an optimal coordinated method for electric vehicles (EVs) participating in frequency regulation (FR) under different power system operation states (PSOSs). In the proposed methodology, the FR power of EVs and generators is coordinated with different optimization objectives for power system secure and economic operations. When a power system operates in normal state, the minimum FR cost is used as an optimization objective considering the battery degradation cost. In the abnormal state, the minimum frequency restoring time is considered in the optimization objective. Based on the optimized results in different scenarios, the output power coordinated control rule between EVs and generators is drawn. Simulations on an interconnected two-area power system have validated the superiority of the proposed optimized coordinated control strategy.

**INDEX TERMS** Electric vehicles, frequency regulation, operation state, coordinated control, vehicle-to-grid.

## I. INTRODUCTION

In order to reduce exhaust emissions and protect environment, many countries encourage renewable energy generation [1]. In the future, renewable energy sources will be massively integrated into power grids and the power system will face serious challenges. Due to the intermittency and uncertainty of renewable energy sources, it is difficult to meet the supply-demand match by only relying on the traditional FR resources [2]. EVs are considered as energy storage devices [3], [4]. Based on vehicle-to-grid (V2G) technology, EVs could charge/discharge from/to power grids [1]. The V2G power in United States, UK, Germany, Italy, etc. may reach 6.8-10 times of their average national load [5], [6], and the number of EVs in the United States has reached 1 million [7]. The increasing number of EVs will bring new opportunities to FR of power system.

There are three ways for EVs participating in FR. The first way is the localized decision-making, for which, each charger determines how much charging/discharging power is based on local information, such as load fluctuations, the arrival time of each EV and the local frequency information

[8], [9]. The second way is the decentralized decision-making. In this case, the FR signals are sent to the aggregators by control center for controlling each charging device based on the operating voltage, power loss and so on [6], [10], [11]. The last way is the centralized decision-making. With the support of the communication system, the chargers are controlled by the control center [7], [12].

In the current literature, there are different optimization objectives for EVs participating in FR such as reducing frequency deviation (FD), improving FR revenue and EV owners' satisfaction [13]-[18]. In order to reduce the FD, the coordinated control strategies of different FR resources are proposed and have better performance [19], [20]. This is because these strategies can utilize the complementarity of different FR resources efficiently. When an operation power system is safe enough, the FR revenue could be improved. The charging/discharging time of EVs could be optimized, for example, EVs charge/discharge from/to grid when the electricity price is low/high [20]-[22]. FR cost reduction, such as reducing the battery degradation cost, also could improve FR revenue [9], [23]. From the EV owners' point of view, their driving requirements are important and should be

satisfied. Therefore, the state-of-charge (SOC) of EV batteries is necessary to be maximized [24], [25].

The PSOSs could be divided into five states based on the security level [26]-[28]. The optimization objectives of power system depend on the PSOS [29]-[31]. For different optimization objectives, the utilization of each FR resource is different. This is because some characteristics of resources are complementary. For example, the response speed of EVs could reach the millisecond level, the thermal power generators and hydroelectric generators just could reach the seconds level. The response speed of EVs is much faster, but the FR cost of them is higher. In our previous research in [13], the response priorities for EVs participating in FR under different PSOSs are involved. EVs participate in FR under different PSOSs is investigated, but the optimal model is not yet established.

In this paper, an optimal coordinated method for EVs participating in FR under different PSOSs is proposed. In the proposed methodology, the FR power of EVs and generators is coordinated with different optimization objectives for power system secure and economic operations. When a power system operates in normal state, the minimum FR cost is used as an optimization objective considering the battery degradation cost. In the abnormal state, the minimum frequency restoring time is considered in the optimization objective. In simulation, a series of random load and step load are added in the normal state and abnormal state respectively. Based on the proposed optimization method, the coordinated control rule between EVs and generators is drawn. The remainder of this paper is arranged as follows. The optimized model is established in Section II. The particle swarm optimization algorithm and the fuzzy set theory are employed to resolve the optimal model in Section III. In Section IV, the proposed coordinated control strategy between EVs and generators is validated. In Section V, the conclusion is made.

## II. PROBLEM FORMULATION

An operation power system should maintain balance between generation and load. Any generation-load mismatch will result in FD. When the system operates in a relatively safe state, the FD is within a certain small range. As the operation power system is divided five states, only normal state is considered relatively safe [27]-[29]. In this paper, the normal state is classified as normal state, and the others are classified as abnormal state.

### A. OBJECTIVE FUNCTION

The formulas on FD is adopted from [6], [30], as shown in (1).

$$\Delta \dot{f} = \frac{1}{M} (\Delta P_{V2G} + \Delta P_{FRR} - \Delta P_L - D\Delta f) \quad (1)$$

$$\Delta P_{V2G} = \sum_{i=1}^N \Delta P_{EV,i} \quad (2)$$

where  $\Delta$  denotes the deviation from the initial steady state;  $f$  is the system frequency;  $M$  is the angular momentum;  $P_{V2G}$  is the aggregated V2G power of all EVs;  $P_{FRR}$  is the output power of other FR resources;  $P_L$  is the frequency nonsensitive

load power;  $D$  is the load-damping coefficient;  $P_{EV,i}$  is the V2G power of the  $i$ th EV;  $N$  is the number of the EVs. In this paper, the EVs are assumed stay in the charging station for the most of time every day. The number of EVs participating in FR could be ensured through incentive measures or policies such as economic incentive. It is similar to demand response (DR). DR is often a cost effective technique that can provide the flexibility required to time shift loads either through prices or incentive policies [21].

The FR cost is formulated as follows:

$$C = C_{EV} + C_m \quad (3)$$

$$C_{EV} = C_{deg} + C_{char} + C_{loss} \quad (4)$$

where  $C$  is the FR cost;  $C_m$  is the FR cost of generators;  $C_{EV}$  is the FR cost of EVs, it consists of battery degradation cost  $C_{deg}$ , charging cost  $C_{char}$  and power loss cost  $C_{loss}$ ;  $C_{char}$  is the cost for purchasing/selling the power from/to the power grid;  $C_{loss}$  is the cost for power transmission loss.

The battery degradation cost is result from the charging/discharging of EV batteries and it is calculated as (5) [12].

$$C_{deg} = \sum_{i \in I} \sum_{t \in W} \alpha P_{EV,it}^2 + \sum_{i \in I} \sum_{t=2}^{|W|} \beta \Delta P_{EV,it}^2 \quad (5)$$

where  $\alpha$  and  $\beta$  are the model parameters;  $P_{EV,it}$  is the charging power and  $\Delta P_{EV,it}$  is the charging power fluctuation of the  $i$ th EV in interval  $t$ ;  $W$  is the interval set;  $I$  is the set of EVs;  $P_{EV,it}$  and  $\Delta P_{EV,it}$  could affect battery temperature and active material of battery, they will result in more battery degradation cost.

When a power system operates in a relatively safe state, the FR cost can be considered to reduce. The objective function is shown as follows:

$$\begin{cases} \min \{ \Delta f_{\max}^f, \Delta f_{\text{aver}}^f, C \}, S_{\text{late}} = 0 \\ \min \{ \Delta f_{\max}^f, \Delta f_{\text{aver}}^f, t_F \}, S_{\text{late}} = 1 \end{cases} \quad (6)$$

where  $\Delta f_{\max}^f$  and  $\Delta f_{\text{aver}}^f$  are the maximum and the average FD values during FR process, respectively;  $t_F$  is the time that the FD restores to normal range;  $S_{\text{late}}$  is the PSOS, when the system operates in normal state it equals 0, otherwise it equals 1.

### B. FR CHARACTERISTICS

#### 1) DYNAMIC CHARACTERISTICS

The dynamic characteristics of generators mainly depend on the time constants of inlet steam chest, reheater and governor. The dynamic characteristics of EVs mainly depend on time constant of battery power adjustment (it can reach up to tens of milliseconds [6], [33]). The response speed and FR accuracy advantages will be obvious if the number of EVs is sufficient. Otherwise the output power of EVs will be restricted by capacity constraint. The output power of the generator is restricted by response speed and ramp rate, compared with that of EVs.

#### 2) COST CHARACTERISTIC

The FR cost of EVs includes battery degradation cost, charging cost and power loss cost. The charging cost is affected by electricity price and charging power, which is expressed as (7). It is a positive number when EVs are charging and a

negative number when EVs are discharging. In this paper, the charging power and discharging power which are provided for FR, are assumed to be equal. If the electricity price for purchasing and selling are also assumed to be equal, the charging cost will be zero. Therefore, the charging cost is not considered in this paper. The power loss cost results from transmission loss and is reflected in charging/discharging efficiency, which is shown in (14) and (15).

$$C_{EVcharge} = \sum_{i \in I} \sum_{t \in W} (P_{charge, it} z_{purchase, t} - P_{discharge, it} z_{sell, t}) \quad (7)$$

where  $P_{charge, it}$  and  $P_{discharge, it}$  are the charging power and discharging power of the  $i$ th EV in interval  $t$  respectively;  $Z_{purchase, t}$  and  $Z_{sell, t}$  are the electricity price for purchasing power from grid and selling power to grid in interval  $t$  respectively.

EV battery has limited cycle life because of the fading of active materials caused by the charging and discharging cycles [36]. This cycle aging is caused by the growth of cracks in the active materials, a process similar to fatigue in materials subjected to cyclic mechanical loading [36], [37]. The influence factors can be summarized as ambient temperature, cycle depth, charging/discharging power and so on. In [12], [36] and [39], the variable of battery degradation cost equations is V2G power. It could be presumed that the equations are established for the ideal operating conditions (for example, the ambient temperature is 25 °C). The relationships between battery degradation cost and V2G power are shown in Fig. 1. The Model 1, Model 2 and Model 3 are battery degradation costs which are calculated based on [12], [36] and [38], respectively. In Model 2, the cost function is a piecewise function, the V2G power in each segment is random. In Model 3, the correlation parameters are the average values. In order to simplify the cost calculation, the cost equation of Model 1 is applied in this paper.

The battery degradation cost, which is shown as (5), is related to the total and the fluctuation of output power of EVs during  $t$ . Over-charging/discharging or over-frequent charging/discharging will shorten service life of the battery. The battery degradation cost is illustrated in Fig. 2, in which charging power indicates FR power of EVs within time  $t$ . It can be seen that the more EVs participate in FR, the lower battery degradation cost is. In Fig. 2, battery capacity limit is not considered, and it is assumed that the charging power of each EV is the same no matter how many EVs participate in FR.

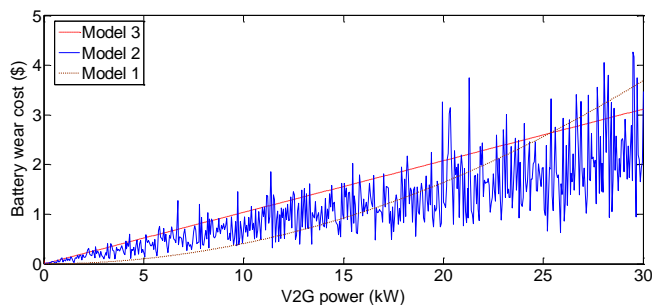


FIGURE 1. The battery degradation cost of EVs

FR cost of generators is shown in (8) [32].

$$\begin{aligned} C_m &= \sum_{g=g_s}^{g_e} \sum_{t=t_s}^{t_e} C_{gt} + \sum_{g=g_s}^{g_e} \sum_{t=t_s}^{t_e} q_{pr, gt} r_{pr, gt} \\ &= \sum_{g=g_s}^{g_e} \sum_{t=t_s}^{t_e} \left[ u_{gt} C_{fix, gt} + a_g G_{gt} + \frac{1}{2} b_g (G_{gt})^2 \right] + \sum_{g=g_s}^{g_e} \sum_{t=t_s}^{t_e} q_{pr, gt} r_{pr, gt} \end{aligned} \quad (8)$$

where  $C_{gt}$  is the running generation cost of the  $g$ th generator during time period  $t$ ;  $t_s$  is the start time of the generator participating in FR;  $t_e$  is the end time of the generator participating in FR;  $u_{gt}$  equals to 1 if the  $g$ th generator is on during time period  $t$  and to 0 if not;  $C_{fix, gt}$  is the  $g$ th generator fixed generation cost during  $t$ ;  $a_g$  and  $b_g$  are the generation cost parameters;  $G_{gt}$  is scheduled generation of the  $g$ th generator in the pre-contingency state during  $t$ ;  $q_{pr, gt}$  is the  $g$ th generator primary reserve rate during  $t$ ;  $r_{pr, gt}$  is scheduled primary reserve of the  $g$ th generator during  $t$ . As can be seen from (8), FR cost of generators is related to output power, generator number and reserve capacity.

### C. CONSTRAINTS

#### 1) SOCS OF EVS

When EVs participate in FR, the SOC should be considered. It affects the charging/discharging capacity of each EV.

$$SOC_{min} \leq SOC_{ini, i} \leq SOC_{max} \quad (9)$$

$$E_{c, i} = (SOC_{max} - SOC_{ini, i}) E_{0, i} \quad (10)$$

$$E_{d, i} = (SOC_{ini, i} - SOC_{min}) E_{0, i} \quad (11)$$

where  $SOC_{max}$  and  $SOC_{min}$  are the maximum and minimum SOC of the EVs respectively; These settings are used for avoiding the batteries over-charging/discharging;  $SOC_{ini, i}$  is the initial SOC of the  $i$ th EV;  $E_{c, i}$  is the energy of the  $i$ th EV for charging;  $E_{d, i}$  is the energy of the  $i$ th EV for discharging;  $E_{0, i}$  is the rated capacity of the  $i$ th EV battery.

#### 2) GENERATOR POWER OUTPUT

In order to avoid the output power of generators is too large or too small, the constraint is shown as (12).

$$\Delta P_{min, m, g} \leq \Delta P_{m, g} \leq \Delta P_{max, m, g} \quad (12)$$

where  $\Delta P_{min, m, g}$  is the minimum output power of the  $g$ th generator participating in FR and  $\Delta P_{max, m, g}$  is the maximum output power of the  $g$ th generator.

#### 3) EV CHARGING/DISCHARGING POWER

As the output power of generators, the constraints for output power of EVs can be expressed as follows:

$$\Delta P_{max, D, i} \leq \Delta P_{V2G, i} \leq \Delta P_{max, C, i} \quad (13)$$

$$\Delta P_{V2GD, i} = \kappa \cdot K_{i, k}^{Down} \cdot \Delta P_{V2GD, i}^* \quad (14)$$

$$\Delta P_{V2GC, i} = \zeta \cdot K_{i, k}^{Up} \cdot \Delta P_{V2GC, i}^* \quad (15)$$

$$P_{sti, down} \leq \sum_{i=1}^{N_{EV}} \Delta P_{V2G, i} \leq P_{sti, up} \quad (16)$$

where  $\Delta P_{max, D, i}$  is the maximum discharging power of the  $i$ th EV during time period  $t$ ;  $\Delta P_{max, C, i}$  is the maximum charging power of the  $i$ th EV during time period  $t$ ;  $\Delta P_{V2GD, i}$  and  $\Delta P_{V2GC, i}$  are actual discharging power and charging power of the  $i$ th EV;  $\zeta$  and  $\kappa$  are the transmission loss efficiency

coefficients. They are both less than 1.  $K_{i,k}^{Down}$  and  $K_{i,k}^{Up}$  are the discharging efficiency and charging efficiency coefficients, respectively;  $\Delta P_{V2GD,i}$  and  $\Delta P_{V2GC,i}$  are the discharging and charging power of the  $i$ th EV;  $P_{sti,down}$  and  $P_{sti,up}$  are the lower and upper limit capacity of the  $sti$ th charging station, respectively.  $N_{EV}$  is the number of EVs stay in charging station.  $\Delta P_{V2GD,i}$  and  $\Delta P_{V2GC,i}$  are vary with the SOC of the  $i$ th EV, which is formulated as (17) - (20) and shown as Fig.3 [14].

$$\begin{cases} K_{i,k}^{Down} = 1 \\ K_{i,k}^{Up} = 0 \end{cases}, SOC_{i,k} \leq SOC_i^{\min} \quad (17)$$

$$\begin{cases} K_{i,k}^{Down} = 0 \\ K_{i,k}^{Up} = 1 \end{cases}, SOC_{i,k} \geq SOC_i^{\max} \quad (18)$$

$$\begin{cases} K_{i,k}^{Down} = \frac{1}{2} \left( 1 + \sqrt{\frac{SOC_{i,k} - SOC_i^{\min}}{SOC_i^{\min} - SOC_i^{\max}}} \right) \\ K_{i,k}^{Up} = \frac{1}{2} \left( 1 - \sqrt{\frac{SOC_{i,k} - SOC_i^{\min}}{SOC_i^{\min} - SOC_i^{\max}}} \right) \end{cases}, SOC_i^{\min} \leq SOC_{i,k} \leq SOC_i^{\max} \quad (19)$$

$$\begin{cases} K_{i,k}^{Down} = \frac{1}{2} \left( 1 - \sqrt{\frac{SOC_{i,k} - SOC_i^{\min}}{SOC_i^{\max} - SOC_i^{\min}}} \right) \\ K_{i,k}^{Up} = \frac{1}{2} \left( 1 + \sqrt{\frac{SOC_{i,k} - SOC_i^{\min}}{SOC_i^{\max} - SOC_i^{\min}}} \right) \end{cases}, SOC_i^{\min} \leq SOC_{i,k} \leq SOC_i^{\max} \quad (20)$$

where  $SOC_i^{\max}$  is the maximum SOC of the  $i$ th EV;  $SOC_i^{\min}$  is the minimum SOC of the  $i$ th EV;  $SOC_i^{\max}$  is the initial SOC of the  $i$ th EV at plug-in time.

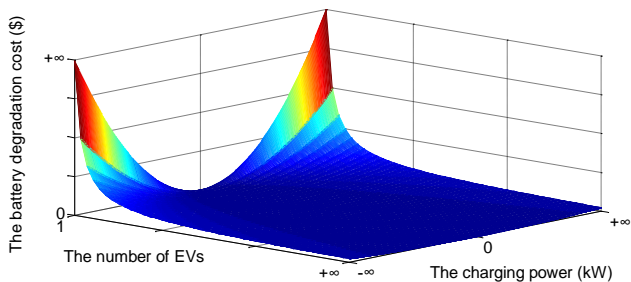


FIGURE 2. Surface chart of battery degradation cost

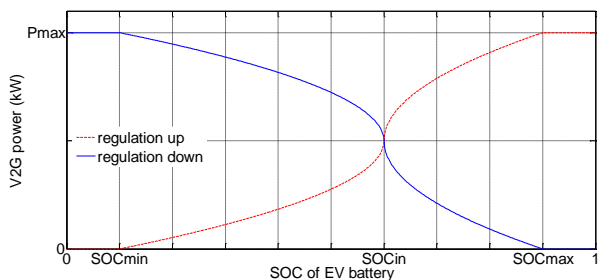


FIGURE 3. The output powers for different SOC EVs

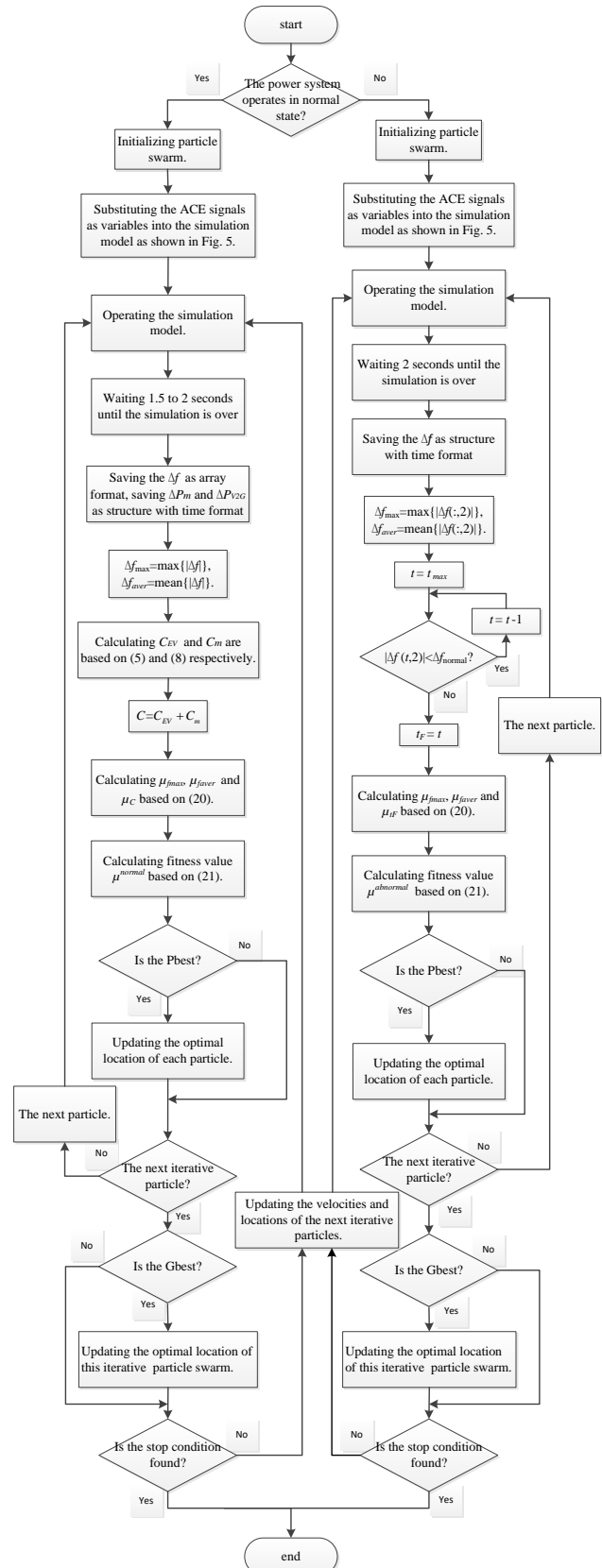


FIGURE 4. The flow chart of optimization procedures

### III. OPTIMIZATION ALGORITHM

After the comparison among particle swarm optimization (PSO) algorithm, genetic algorithm (GA) and evolutionary

algorithms (EAS), the optimization result of PSO is overall best. In this paper, the PSO algorithm is chosen. The fuzzy set theory is employed in this paper to find the best compromise solution. The solution procedures are shown as (21) and (22) [34]. The  $e$ th objective function of a solution in the set  $F_e$  is represented by a membership function  $\mu_e$ . The flow chart of the optimization procedures is shown in Fig. 4.

$$\mu_e = \begin{cases} 1, & |F_e| \leq |F_e|_{\min} \\ \frac{|F_e|_{\max} - |F_e|}{|F_e|_{\max} - |F_e|_{\min}}, & |F_e|_{\min} < |F_e| < |F_e|_{\max} \\ 0, & |F_e| \geq |F_e|_{\max} \end{cases} \quad (21)$$

$$\mu^\theta = \frac{\sum_{e=1}^{N_{obj}} \xi_e \mu_e^\theta}{\sum_{h=1}^H \sum_{e=1}^{N_{obj}} \xi_e \mu_e^h} \quad (22)$$

where  $|F_e|_{\max}$  and  $|F_e|_{\min}$  are the maximum and minimum value of the  $e$ th objective function respectively. For each solution  $\theta$ , the normalized membership function  $\mu_\theta$  is calculated as (22).  $H$  is the number of solutions. The best compromise solution is the one with the maximum  $\mu_\theta$ .  $\xi_e$  is the weight coefficient of the  $e$ th objective function.

#### IV. SIMULATIONS AND RESULTS

In this paper, the proposed approach is an off-line optimization to determine the optimal coordinated control strategy for EVs and generators participating in FR. The off-line optimization process should be implemented with a great variety of load disturbances to experience enough power system scenarios in a high-accuracy simulation environment, and numerous explorations with EV charging/discharging strategies should be sampled sufficiently in various system operation states. Consequently, the optimized control strategy can then be implemented for on-site operation, and the optimal charging/discharging power for each EV can be obtained to meet the timeliness requirement based on the current system operation state.

The simulation model based on MATLAB/Simulink is shown as Fig. 5. The FR resources of both area A and area B include generators and EVs. The model parameters of the two-area interconnected system are taken from [6] and [13], as shown in Table I-III. The FR signal is based on the area control error (ACE) under the TBC control mode, as follows,

$$ACE = \Delta P_{tie} + B\Delta f \quad (23)$$

In order to simulate the load fluctuation in normal state, a series of random load, which fluctuates within a certain range, is added in area A and area B. As the unit of the parameters in Table IV is hour, the random fluctuation time of the load in normal state is set to 1 hour. Two step loads are added in area A and area B respectively, for simulating the disturbed load in abnormal state of power system, one is -0.8MW the other is  $P_{abnormal}$ .

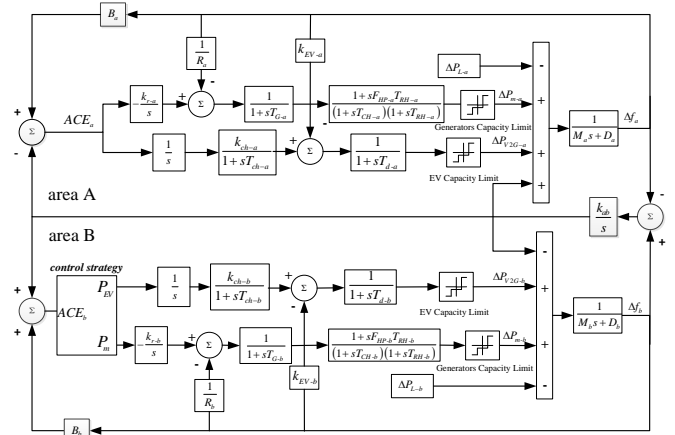


FIGURE 5. Block diagram of FR for two areas with generators and EV charging stations

TABLE I PARAMETERS OF THE SIMULATION SYSTEM MODEL

Parameters	Value	Parameters	Value
System base (MW)	10	Nominal frequency (Hz)	60
$T_{G-a}, T_{G-b}$ (sec)	0.5	$D_a, D_b$ (MW/Hz)	1/6
$T_{CH-a}, T_{CH-b}$	0.8	$R_a, R_b$ (Hz/MW)	0.3
$T_{RH-a}, T_{RH-b}$ (sec)	10	$k_{r-a}, k_{r-b}$ (MW/Hz/sec)	2/15
$M_{a1}, M_{b1}$ (MW/Hz/s)	2.0	$F_{HP-a}, F_{HP-b}$	30%

TABLE II PARAMETERS OF THE EV CHARGING STATION MODEL

Parameters	Value
EV frequency characteristic coefficient, $k_{ev-a}, k_{ev-b}$ (MW/Hz)	1.12
EV battery gain, $k_{ch-a}, k_{ch-b}$	1
EV battery filter time constant, $T_{ch-a}, T_{ch-b}$ (sec)	1
1st order delay of DC/AC converter, $T_{d-a}, T_{d-b}$ (sec)	2
The number of EVs in area A	817
The number of EVs in area B	817
The number of generators in area A	1
The number of generators in area B	1

#### A. OPTIMIZATION AND ANALYSIS OF CONTROL STRATEGY

In this paper, the multiples of FR capacity allocated for EVs and generators, express as the ace signals for EVs and generators, are the decision variables. The relevant parameters are shown in Table IV [12]. The optimization objectives in different states are formulated as (6).

TABLE III PARAMETERS OF EVS

Parameters	Value	SOC of EVs	Number
$SOC_{\min}$	0.1	0.9	41
$SOC_{\max}$	0.9	0.8	67
$SOC_{io}$	0.6	0.7	90
Battery capacity (kWh)	50	0.6	270
$\Delta P_{\max D,i}$	25	0.5	100
$\Delta P_{\max C,i}$	25	0.4	80
$\kappa$	0.8	0.3	60
$\zeta$	0.8	0.2	27
		0.1	32

TABLE IV THE FR COST PARAMETERS

Parameters	Value	Parameters	Value
$C_{it}$ (\$/h)	10	Number of particles	100
$a_{it}$ (\$/MWh)	9.8	Number of iterations	100
$b_{it}$ (\$/MWh <sup>2</sup> )	0	$v_x m_j, v_x EV_j$	[-1,1]
$q_{pr,it}$ (\$/MWh)	10	$c1, c2$	0.8
$\alpha$ (\$/KWh <sup>2</sup> )	$3.826 \times 10^{-4}$	$r1, r2$	random[0,1]
$\beta$ (\$/KWh <sup>2</sup> )	$7.652 \times 10^{-4}$	$\omega_m, \omega_{EV}$	1
$\xi_{normal-fmax}$	1	$\xi_{abnormal-faverage}$	1
$\xi_{normal-faverage}$	1	$\xi_{abnormal-faverage}$	1
$\xi_{normal-cost}$	1	$\xi_{abnormal-t}$	1

## 1) NORMAL STATE

As shown in Fig. 6 and Fig. 7, the sum of output power of EVs and generators in normal state fluctuates significantly because of the random loads. The sum output power of EVs and generators in normal state trends to increase with the increase of  $P_{normal}$ . The sum output power of EVs is small, and the output power at each moment can be negligible.

## 2) ABNORMAL STATE

In the abnormal state, the operation power system is not safe. In order to make the FD restore to the normal range as soon as possible, the complementary of EVs and generators should be utilized. As shown in Fig. 8 and Fig. 9, in abnormal state, the output power of generators increases with the increase of  $P_{abnormal}$  and the output power of EVs is always the maximum. The output power is the final stable value. In abnormal state, the optimized effect of any of these three objectives is the same, the minimum FD. Therefore, the output power has no rule with the  $\xi_{abnormal-t}$ .

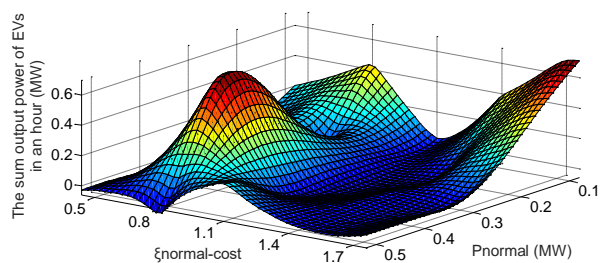


FIGURE 6. The sum output power of EVs under different scenarios in normal state

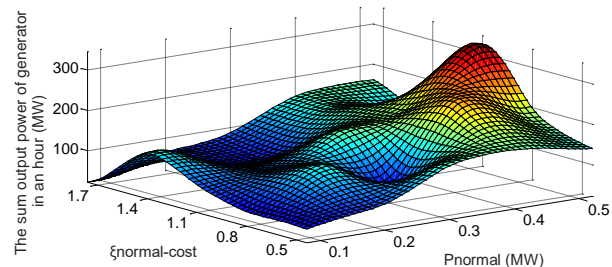


FIGURE 7. The sum output power of generators under different scenarios in normal state

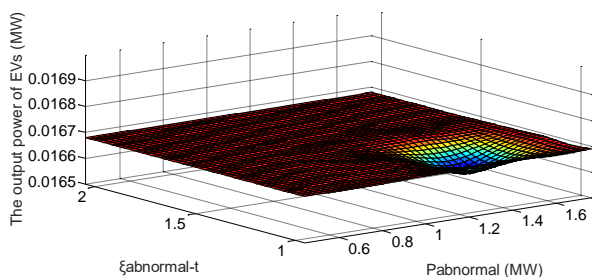


FIGURE 8. The output power of EVs under different scenarios of abnormal state  
In normal state, the output power of EVs can be negligible. In abnormal state, the output power of EVs is the maximum. The respond speed and FR accuracy of EVs, and the FR capacity of generators, are effectively utilized. The FR cost is considered.

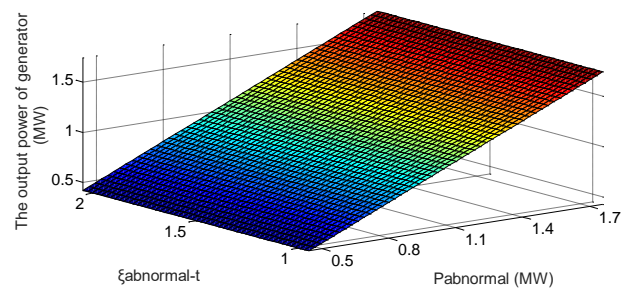


FIGURE 9. The output power of generators under different scenarios of abnormal state

## B. SIMULATION AND DISCUSSION

The FR strategy, which is shown in area A of Fig. 5, is named STRATEGY1. As shown in [13], the FR control strategy is named STRATEGY2. In STRATEGY2, the response priorities and control strategies for the FRRs vary with different operating states. The FR control strategy optimized by the proposed optimization method, which is shown in Table V, is named STRATEGY3. In STRATEGY3, the number of EVs is increased to two times, is named STRATEGY3+.

In order to evaluate the effectiveness of the FR control strategies, the different indicators in different states are calculated and listed in Tables VI.

## 1) NORMAL STATE

TABLE V THE COORDINATED CONTROL STRATEGY3

	Normal state	Abnormal state
$P_{EV}$	$0*ACE$	$2*ACE$
$P_m$	$0.6*ACE$	$2*ACE$

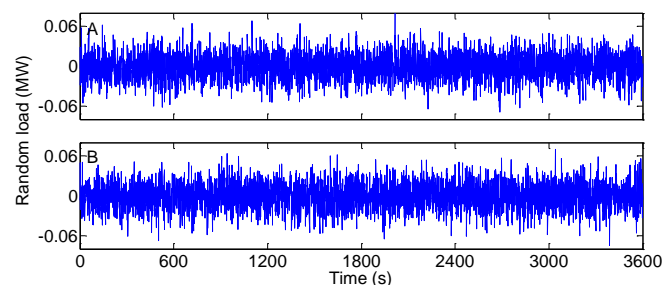


FIGURE 10. Random loads fluctuation within one hour in area A (A) and in area B (B)

The random load is assumed to be under the normal distribution [40]-[42], and it is formulated as (24) and is simulated as Fig. 10.

$$P_{random}(t) = \mu + P_{normal} \cdot \sigma \cdot randn \quad (24)$$

where  $P_{random}$  is the load fluctuation in normal state;  $\mu$  and  $\sigma$  are parameters of the normal distribution function, they equal to 0 and 0.388.  $P_{normal}$  is the maximum value of the load fluctuation in the most of time, it equals to 0.06 MW in Fig. 10;  $randn$  is a standard normal distribution random number in [0,1].

The output power of different control strategies is shown in Fig. 11. In STRATEGY1 and STRATEGY2, the EVs and

generators participate in FR. In STRATEGY3, only the generators undertake the FR task. In STRATEGY3, the output power of generators is the least.

Tie-line power of different control strategies is shown in Fig. 12. In STRATEGY3, the tie-line power fluctuation is more dramatic than STRATEGY1 and STRATEGY2. This is because the FR power in STRATEGY3 is the least.

The FD of different coordinated control strategies is shown in Fig. 13. The FR power in STRATEGY3 is the least. However, the FD of STRATEGY3 is a little less than other strategies. As shown in Table VI, the FR effect of STRATEGY3 is the best, and the FR cost is much less than other strategies. This is because the random load fluctuates constantly. The FR cost of STRATEGY2 is less than that of STRATEGY2. This is because the output power of generators in STRATEGY3 is the less. The FR result of STRATEGY3+ is the same with STRATEGY3, this is because EVs do not participate in FR.

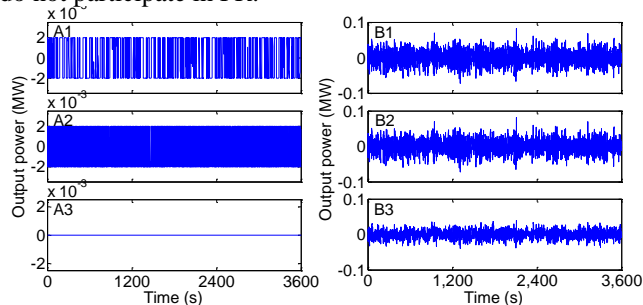


FIGURE 11. The output power of EVs with STRATEGY1 (A1), of generators with STRATEGY2 (B1), of EVs with STRATEGY2 (A2), of generators with STRATEGY2 (B2), of EVs with STRATEGY3 (A3) and of generators with STRATEGY3 (B3) in the normal state

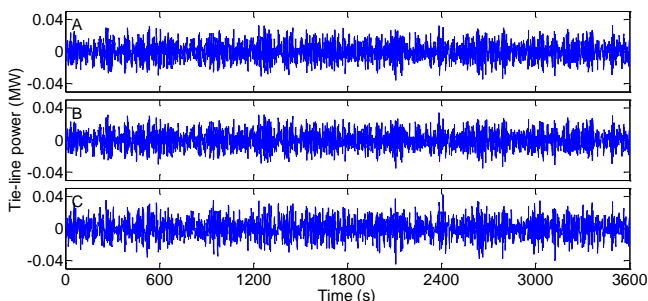


FIGURE 12. The tie-line power with STRATEGY1 (A), with STRATEGY2 (B) and with STRATEGY3 (C) in the normal state

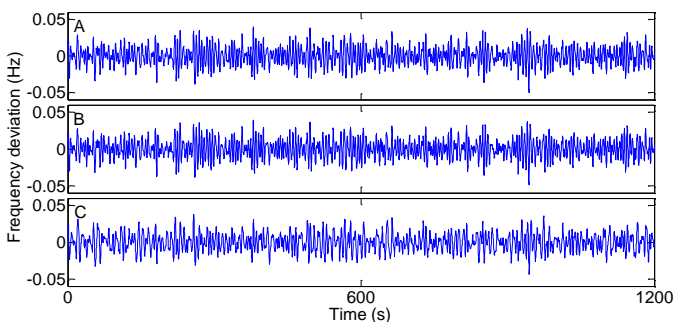


FIGURE 13. The FD with STRATEGY1 (A), with STRATEGY2 (B) and STRATEGY3 (C) in the normal state

## 2) ABNORMAL STATE

A -0.8MW load and an 1.6MW load are added in area A at the 10<sup>th</sup> second and area B at the 15<sup>th</sup> second respectively. The output power of different strategies is shown as Fig. 14. In STRATEGY2, EVs participate FR when the ACE reaches response thresholds. In STRATEGY3, the output power of EVs response faster than STRATEGY1 and STRATEGY2.

The tie-line power and FD of different strategies are shown in Fig. 15 and Fig. 16 respectively. As shown in Table VI, the performance of STRATEGY3 is the best, and the performance of STRATEGY3+ is better than STRATEGY3 because that there are more EVs participating in FR and more quick response power. The performance of STRATEGY3+ is a little better because of the capacity constraint of EVs.

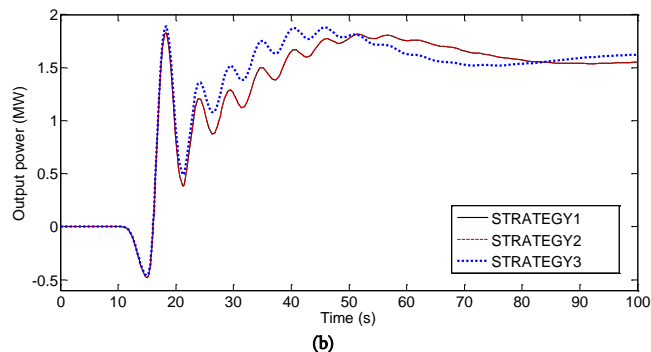
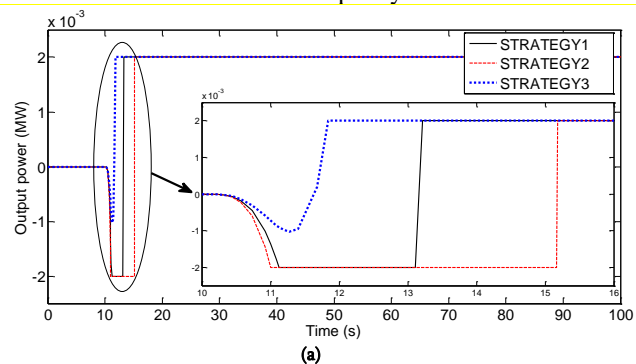


FIGURE 14. The output power of EVs (a) and generators (b) with strategies in the abnormal state

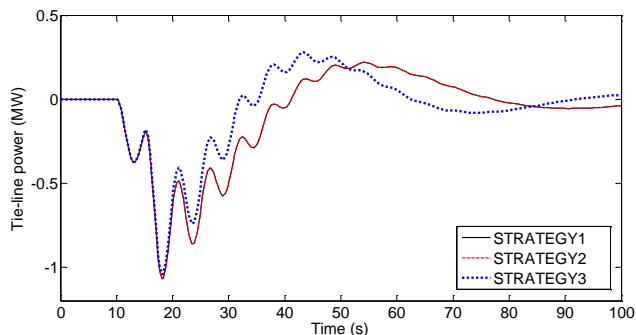


FIGURE 15. The tie-line power with strategies in the abnormal operating state  
In the normal state, the power system is operating in a relatively safe state and the FD fluctuates within a certain range. Therefore, the output power of FR resources could be less for FR cost reduction. In the abnormal state, the only goal is to improve system security. Therefore, the response speed and FR accuracy advantages of EVs should be utilized.



Based on the optimized results, the output power of generators is appropriately less and the output power of EVs is as less as possible in normal state, and the output power of EVs is as much as possible and the remainder of the FR power is the output power of generators in abnormal state.

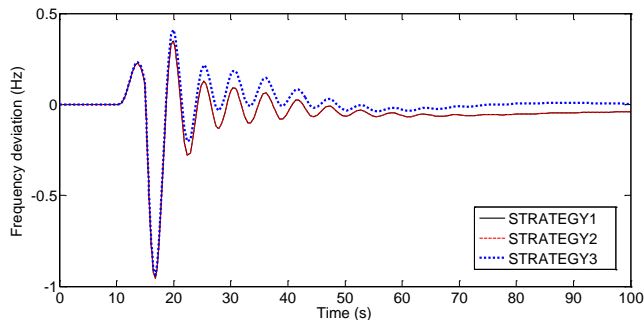


FIGURE 16. The FD with strategies in the abnormal operating state

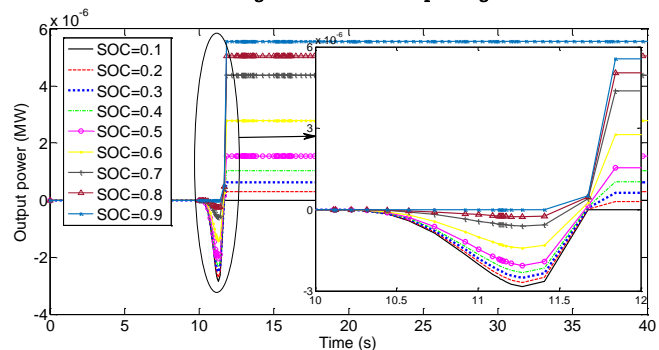


FIGURE 17. The output powers for different SOC EVs in abnormal state

TABLE VI SIMULATION RESULTS OF DIFFERENT METHODS

	STRATEGY1	STRATEGY2	STRATEGY3	STRATEGY3+	
The normal state	The maximum FD (Hz)	0.0552	0.0542	0.0549	0.0549
	The average FD (Hz)	0.0120	0.0122	0.0106	0.0106
	The FR cost of generators (\$)	276.1746	211.3497	231.0159	231.0159
	The FR cost of EVs (\$)	541.3750	485.6162	0	0
	The total cost (\$)	817.5496	696.9659	231.0159	231.0159
The abnormal state	The maximum FD (Hz)	0.9557	0.9552	0.9347	0.9346
	The average FD (Hz)	0.0134	0.0134	0.0096	0.0096
	The recovery time (s)	85.1717	85.1716	42.9876	42.9874

## V. CONCLUSION

In this paper, an optimal coordinated method for EVs participating in FR under different PSOSs is proposed. In the proposed methodology, the complementarity of EVs and generators under different PSOSs is utilized. In normal state, the power system is relatively safe, while in the abnormal state, the FD must be restored to normal range as soon as possible. When a power system operates in normal state, the minimum FR cost is used as an optimization objective considering the battery degradation cost. In the abnormal state, the minimum frequency restoring time is considered in the optimization objective. In this paper, the FR cost of EVs is higher but the response speed is more rapidly. In the simulation examples, a series of random load in an hour and step load are added as disturbed loads. Based on the optimized results in different scenarios, the optimal coordinated control rule between EVs and generators is drawn. The output power of EVs and generators is suggested to be less in normal state and the output power of EVs is suggested to be more in abnormal state. The simulation results have proved that the FR cost is reduced in normal state and the frequency recovery time and the FD are improved in abnormal state with the proposed coordinated method.

## REFERENCES

[1] Y. Mu, J. Wu, J. Ekanayake, N. Jenkins and H. Jia, "Primary frequency response from electric vehicles in the Great Britain power system," *IEEE Trans. Smart Grid*, vol. 4, no. 2, pp. 1142-1150, Jun. 2013.

[2] H. Liu, J. Qi, J. Wang, P. Li, C. Li, and H. Wei, "EV dispatch control for supplementary frequency regulation considering the expectation of EV owners," *IEEE Trans. Smart Grid*, vol. 9, no. 4, pp. 3763-3772, Jul. 2018.

[3] A. Jensen, S. Mabit, "The use of electric vehicles: a case study on adding an electric car to a household," *Transportation Research Part A-Policy and Practice*, vol. 106, pp. 89-99, Dec. 2017.

[4] M. Tushar, A. Zeineddine, C. Assi, "Demand-side management by regulating charging and discharging of the EV, ESS, and utilizing renewable energy," *IEEE Trans Industrial Informatics*, vol. 14, no. 1, pp. 117-126, Sep. 2018.

[5] W. Kempton and A. Dhanju, "Electric vehicles with V2G: Storage for large-scale wind power," *Windtech International*, vol. 2, no. 2, pp. 18-21, Mar. 2006.

[6] H. Yang, C. Chung and J. Zhao, "Application of plug-in electric vehicles to frequency regulation based on distributed signal acquisition via limited communication," *IEEE Trans. Power Systems*, vol. 28, no. 2, pp. 1017-1026, May. 2013.

[7] M. Arias, M. Kim, S. Bae, "Prediction of electric vehicle charging-power demand in realistic urban traffic networks," *Applied Energy*, vol. 195, pp. 738-753, Jun. 2017.

[8] S. Guner, A. Ozdemir, "Stochastic energy storage capacity model of EV parking lots," *IET Generation Transmission & Distribution*, vol. 11, no. 7, pp. 1754-1761, Jun. 2017.

[9] Y. Cao, S. Yang, G. Min, et al., "A cost-efficient communication framework for battery-switch-based electric vehicle charging," *IEEE Communications Magazine*, vol. 55, no. 1, pp. 162-169, May. 2017.

[10] M. Caramanis, E. Ntakou, W. ogran, et al., "Co-optimization of power and reserves in dynamic T&D power markets with nondispatchable renewable generation and distributed energy resources," *Proceedings of the IEEE*, vol. 104, no. 4, pp. 807-836, Mar. 2016.

[11] K. Ko, D. Sung, "The effect of EV aggregators with time-varying delays on the stability of a load frequency control system," *IEEE Trans. Power Systems*, vol. 33, no. 1, pp. 669-680, Apr. 2018.

[12] Y. F. He, B. Venkatesh and L. Guan, "Optimal scheduling for charging and discharging of electric vehicles," *IEEE Trans. Smart Grid*, vol. 3, no. 3, pp. 1095-1105, Sep. 2012.

- [13] J. Zhong, L. He, C. Li, Y. Cao, J. Wang, B. Fang, L. Zeng and G. Xiao, "Coordinated control for large-scale EV charging facilities and energy storage devices participating in frequency regulation," *Applied Energy*, vol. 123, no. 12, pp. 253-262, Jun. 2014.
- [14] H. Liu, Z. Hu, Y. Song, J. Wang and X. Xie, "Vehicle-to-grid control for supplementary frequency regulation considering charging demands," *IEEE Trans. Power Systems*, vol. 30, no. 6, pp. 3110-3119, Nov. 2015.
- [15] I. Pavic, T. Capuder, I. Kuzle, "Value of flexible electric vehicles in providing spinning reserve services," *Applied Energy*, vol. 157, pp. 60-74, Nov. 2015.
- [16] D. T. Nguyen and L. B. Le, "Joint optimization of electric vehicle and home energy scheduling considering user comfort preference," *IEEE Trans. Smart Grid*, vol. 5, no. 1, pp. 188-199, Jan. 2014.
- [17] N. DeForest, J. MacDonald, D. Black, "Day ahead optimization of an electric vehicle fleet providing ancillary services in the Los Angeles Air Force Base vehicle-to-grid demonstration," *Applied Energy*, vol. 210, pp. 987-1001, Jan. 2018.
- [18] M. Kazemi, M. Sedighzadeh, M. Mirzaei, O. Homaei, "Optimal siting and sizing of distribution system operator owned EV parking lots," *Applied energy*, vol. 179, pp. 1176-1184, Oct. 2016.
- [19] Y. Lin, P. Barooah, S. Meyn and T. Middelkoop, "Experimental evaluation of frequency regulation from commercial building HVAC systems," *IEEE Trans. Smart Grid*, vol. 6, no. 2, pp. 776-783, Mar. 2015.
- [20] K. Hu, P. Yi and C. M. Liaw, "An EV SRM drive powered by battery/supercapacitor with G2V and V2H/V2G capabilities," *IEEE Trans. Industrial Electronics*, vol. 62, no. 8, pp. 4714-4727, Aug. 2015.
- [21] Q. Chen, F. Wang, B. Hodge, "Dynamic price vector formation model-based automatic demand response strategy for PV-assisted EV charging Stations," *IEEE Trans. Smart Grid*, vol. 8, no. 6, pp. 2903-2915, Apr. 2017.
- [22] D. Dallinger, J. Link and M. Buttner, "Smart grid agent: Plug-in electric vehicle," *IEEE Trans. Sustainable Energy*, vol. 5, no. 3, pp. 710-717, Jul. 2014.
- [23] A. David, I. Al-Anbagi, "EVs for frequency regulation: cost benefit analysis in a smart grid environment," *IET Electrical Systems in Transportation*, vol. 7, no. 4, pp. 310-317, Dec. 2017.
- [24] C. Peng, J. Zou, L. Lian, L. Li, "An optimal dispatching strategy for V2G aggregator participating in supplementary frequency regulation considering EV driving demand and aggregator's benefits," *Applied Energy*, vol. 190, pp. 591-599, Mar. 2017.
- [25] T. Hoogvliet, G. Litjens, S. Van, "Provision of regulating- and reserve power by electric vehicle owners in the Dutch market," *Applied Energy*, vol. 190, pp. 1008-1019, Mar. 2017.
- [26] L. H. Fink and K. Carlsen, "Operating under stress and strain," *IEEE Spectrum*, vol. 15, pp. 48-53, Mar. 1978.
- [27] R. Billinton and E. Khan, "A security based approach to composite power system reliability evaluation," *IEEE Trans. Power Systems*, vol. 7, no. 1, pp. 65-71, Feb. 1992.
- [28] R. J. Marceau, J. Endrenyi, R. Allan, e. al, "Power system security assessment: a position paper," *Electra*, vol. 175, pp. 49-77 no. 2, Dec. 1997.
- [29] M. Kim, "Multi-objective optimization operation with corrective control actions for meshed AC/DC grids including multi-terminal VSC-HVDC," *International Journal of Electrical Power & Energy Systems*, vol. 93, pp. 178-193, Dec. 2017.
- [30] P. Kundur, *Power System Stability and Control*, CA: McGraw-Hill, 1994, pp. 391.
- [31] A. Ogunjuyigbe, T. Ayodele, O. Akinola, "Optimal allocation and sizing of PV/Wind/Split-diesel/Battery hybrid energy system for minimizing life cycle cost, carbon emission and dump energy of remote residential building," *Applied Energy*, vol. 171, no. 6, pp. 153-171, Jun. 2016.
- [32] J. F. Restrepo and F. D. Galiana, "Unit commitment with primary frequency regulation constraints," *IEEE Trans. Power Systems*, vol. 20, no. 4, pp. 1836-1842, Nov. 2005.
- [33] W. Kempton and J. Tomic, "Vehicle-to-grid power implementation: From stabilizing the grid to supporting large-scale renewable energy," *Journal Power Sources*, vol. 144, no. 1, pp. 280-294, 2005.
- [34] Dubarry M., Vuillaume N. and Liaw B. Y, "From single cell model to battery pack simulation for Li-ion batteries," *Journal of Power Sources*, vol. 186, no. 2, pp. 500-507, Jan. 2009.
- [35] Dennis D. W., Battaglia V. S. and Belanger A., "Electrochemical modeling of lithium polymer batteries," *Journal of Power Source*, vol. 110, no. 2, pp. 310-320, Aug. 2002.
- [36] B. Xu, J. Zhao, T. Zheng and D. S. Kirschen, "Factoring the cycle aging cost of batteries participating in electricity markets," *IEEE Trans. Power Systems*, vol. 33, no. 2, pp. 2248-2259, Mar. 2018.
- [37] J. Vetter, P. Novák, M. R. Wagner, C. Veit, K. C. Möller, J. O. Besenhard, M. Winter, M. Wohlfahrt-Mehrens, C. Vogler and A. Hammouch, "Ageing mechanisms in lithium-ion batteries," *J. Power Sources*, vol. 147, no. 1, pp. 269-281, 2005.
- [38] H. Farzin, M. F. Firuzabad and M. M. Aghtaei, "A practical scheme to involve degradation cost of Lithium-Ion batteries in Vehicle-to-Grid applications," *IEEE Trans. Sustainable Energy*, vol. 7, no. 4, pp. 1730-1738, Oct. 2016.
- [39] M. A. Abido, "Multiobjective evolutionary algorithms for electric power dispatch problem," *IEEE Trans. Evolutionary Computation*, vol. 10, no. 3, pp. 315-329, Jun. 2006.
- [40] S. Zhang, H. Cheng, L. Zhang, M. Bazargan, and L. Yao, "Probabilistic evaluation of available load supply capability for distribution system," *IEEE Trans. Power Systems*, vol. 28, no. 3, pp. 3215-3225, Aug. 2013.
- [41] Z. Ren, W. Li, R. Billinton and W. Yan, "Probabilistic Power Flow Analysis Based on the Stochastic Response Surface Method," *IEEE Trans. Power Systems*, vol. 31, no. 3, pp. 2307-2315, May 2016.
- [42] H. Liu, K. Huang, Y. Yang, H. Wei and S. Ma, "Real-time vehicle-to-grid control for frequency regulation with high frequency regulating signal," *Protection and Control of Modern Power Systems*, vol. 3, pp. 13, May 2018.
- [43] S. Xia, S. Q. Bu, X. Luo, K. W. Chan, and X. Lu, "An autonomous real time charging strategy for plug-in electric vehicles to regulate frequency of distribution system with fluctuating wind generation," *IEEE Trans. Sustainable Energy*. (accept)
- [44] W. Su, H. Eichi, W. Zeng, and M. Y. Chow, "A Survey on the Electrification of Transportation in a Smart Grid Environment," *IEEE Trans. Inf. Inform.*, vol. 8, no. 1, pp. 1-10, Feb. 2012.